# Supporting Information

## Liu et al. 10.1073/pnas.1306180110

### SI Materials and Methods

**T-Cell Culture.** The animal protocols used for this study were approved by the Institutional Animal Care and Use Committee of Memorial Sloan-Kettering Cancer Center. $CD4^+$ T cells were isolated from lymph nodes of 5C.C7 αβ T-cell receptor (TCR)-transgenic mice and stimulated with irradiated splenocytes from congenic B10A mice at a ratio of 1:5 in the presence of 5 μM moth cytochrome $c_{88–103}$ (MCC) peptide. Cells were maintained in RPMI medium containing 10% (vol/vol) FCS. IL-2 (30 IU/mL) was added to the cells 16 h after initiation of culture, and cells were split in RPMI medium containing IL-2 (30 IU/mL) as needed. CH12 cells were grown in RPMI medium containing 10% (vol/vol) FCS.

**Signaling Probes.** Full-length coding sequences of dynein light intermediate chain (DynLIC) (dync1li1), Dyn2LIC (dync2li1), TcTex light chain (dynlt1b), centrin 2, and nonmuscle myosin (NM) regulatory light chain (myl12b) were amplified from RNA derived from 5C.C7 T-cell blasts and ligated into a murine stem cell virus (MSCV) retroviral expression vector upstream of and in-frame with either GFP or Tag-RFP-T. Constructs for labeled dynein intermediate chain (DynIC), tubulin, Lifeact, PKCθ, PKCη, and PKCε have been described (1–3). The S1AS2A and T18AS19A mutants of myosin regulatory light chain (MyoRLC) were generated by two-step mutagenesis. In the first step, both the 5′ and 3′ ends of the gene were amplified using primers containing the mutation. Then, the two fragments were joined by a third PCR and ligated into the MSCV vector upstream of GFP.

**shRNA Constructs.** MSCV-LTRmiR30-PIG–based vectors (derived from LMP; Open Biosystems) were used for all shRNA constructs. These vectors each contain a puromycin-resistance marker and a fluorescent protein marker (GFP, RFP, or CFP) for selection of shRNA-transduced cells. shRNA sequences were obtained from Open Biosystems, amplified by PCR, and ligated into the LMP vector. Mature sequences of individual shRNAs were as follows: nontargeting shRNA, 5′-TTACTCTCGCCCAAGCGAG-3′; DynHC (dync1h1) shRNA, 5′-TTAGCTTGAGGACATTCCC-3′; DynIC (dync1i2) shRNA, 5′-AATTTCTGCGAGTGTTCGG-3′; myosin heavy chain (myh9) shRNA, 5′-TAAGCCCTGAGTAGTATCG-3′; PKCη (prkch) shRNA, 5′-ACACTGAAGTCCTTGTCGC-3′; and PKCε (prkce) shRNA, 5′-AACTTGACATTGATATCCC-3′.

**Retroviral Transduction.** shRNAs and signaling probes were retrovirally transduced into T-cell blasts 72 h after initiation of culture as described (1). In shRNA knockdown experiments, 5 μg/mL puromycin (Invitrogen) was added to cells 24 h post-transduction. shRNA-transduced cells were isolated by centrifugation over Histopaque (Sigma) 48 h after puromycin selection.

**Immunoblot Analysis.** shRNA-transduced cells were lysed, and 15–30 μg of total protein was analyzed by immunoblot using the following antibodies: DynHC (1:500; sc-7526-R; Santa Cruz Biotechnology), DynIC (1:500; sc-70997; Santa Cruz Biotechnology), MyH9 (1:5,000; BT-567; Biomedical Technologies), PKCθ (1:500 dilution; sc-212; Santa Cruz Biotechnology), PKCη (1:400 dilution; sc-215; Santa Cruz Biotechnology), and PKCε (1:1,000 dilution; c21; BD Transduction Laboratory). For analysis of T-cell activation, T cells were mixed with CH12 cells loaded with 1 μM MCC peptide at 1:1 ratio, centrifuged briefly to facilitate conjugation, and incubated at 37 °C for different lengths of time. Phosphorylated Erk levels in lysates derived from these cells were assessed using a monoclonal antibody (1:1,000; 20G11; Cell Signaling). All blots were reprobed with anti–β-actin antibody (1:10,000 dilution; AC-15; Sigma) as a loading control.

**GM130 Immunocytochemistry.** T cells were attached to glass slides coated with poly-L-lysine, fixed with 4% paraformaldehyde, permeabilized with 0.2% Triton X-100, and blocked with 5% donkey serum in PBS. Mouse anti-GM130 antibodies conjugated with Alexa 647 (558712; BD Pharmingen) were used to identify the Golgi apparatus. Coverslips were mounted with Vectashield mounting medium (Vector Laboratories) on Superfrost glass slides (Fisher). Fixed cells were imaged with an SP5-upright confocal microscope (Leica) fitted with a 63× objective. Z stacks with 0.5-μm sections were acquired, and maximum projection images were created using SlideBook software (Intelligent Imaging Innovations).

**Live Imaging of Conjugates.** T cells expressing MyoRLC-GFP and centrin-RFP were loaded with Fura-2 acetoxymethyl ester AM (Invitrogen) and transferred into minimal imaging medium in 16-well chamber slides (Invitrogen). Time-lapse imaging began after the addition of MCC-loaded CH12 cells. Brightfield and Fura-2 images, along with a 20-μm z stack of GFP and RFP images, were collected every 30 s for 30 min with a 40× objective lens (Olympus). Maximum projections of GFP and RFP at each time point were created using SlideBook.

**Image Analysis.** Images were analyzed using SlideBook and Matlab (MathWorks), and the data were visualized using Prism (GraphPad). Centrosome polarization in photoactivation experiments was quantified by measuring the mean distance between the centrosome and the center of the UV irradiated region for each time point over an ensemble of cells. Instantaneous speed was calculated by dividing the distance between consecutive centrosome positions by the time interval (3 s). Recruitment or depletion from the irradiated region was quantified by calculating the mean fluorescence intensity (MFI) in the region, after background correction, for each time point, followed by normalization using the 10 time points before photoactivation. Temporal offsets between different events (e.g., NMII depletion and DynIC accumulation) were calculated by cross-correlation analysis as described (1). Cross-correlation values are presented in the text as ±SEM. NMII enrichment at the "back" of the cell (Figs. 3*B* and 7*D*, and Fig. S8*F*) was determined by computing the MyoRLC MFI ratio between the "back" and "front" halves of the cell for each time point. The line passing through the cell center of mass (COM) perpendicular to the vector connecting the COM with the center of the irradiated region was used to divide the cell into "back" and "front" halves, with the "front" half containing the irradiated region. To determine the correlation of centrosome step size with NMII accumulation (Fig. 3*C*), the MyoRLC MFI in the region in front of the centrosome was subtracted from the MyoRLC MFI in the region behind it for each time point. For this analysis, the demarcation between "front" and "back" was the line passing through the centrosome perpendicular to the direction of centrosome motion for that step. For each time point, "back" was defined as the region the centrosome was moving away from. NMII clustering and dispersion in response to acute addition of phorbol myristate acetate (PMA), Gö6983, and Y27632 was quantified by calculating the SD of MyoRLC fluorescence at the cell membrane for each time point. Colocalization was quanti-

fied by calculating the Pearson's correlation coefficient (PCC) for each image after intensity thresholding. To focus on the dominant features in each image (i.e., NMII clusters and dynein accumulation), only pixels in which the fluorescence intensity of either GFP or RFP was >1.05 × the average GFP or RFP fluorescence, respectively, of the cell were used for the PCC calculation. Centrosome polarization in fixed conjugates was assessed by polarization index, defined as the distance between the centrosome and the immunological synapse (IS) divided by the distance between the back of the T cell and the IS.


1. Quann EJ, Merino E, Furuta T, Huse M (2009) Localized diacylglycerol drives the polarization of the microtubule-organizing center in T cells. *Nat Immunol* 10(6):627–635.
2. Quann EJ, Liu X, Altan-Bonnet G, Huse M (2011) A cascade of protein kinase C isozymes promotes cytoskeletal polarization in T cells. *Nat Immunol* 12(7):647–654.
3. Riedl J, et al. (2008) Lifeact: A versatile marker to visualize F-actin. *Nat Methods* 5(7):605–607.


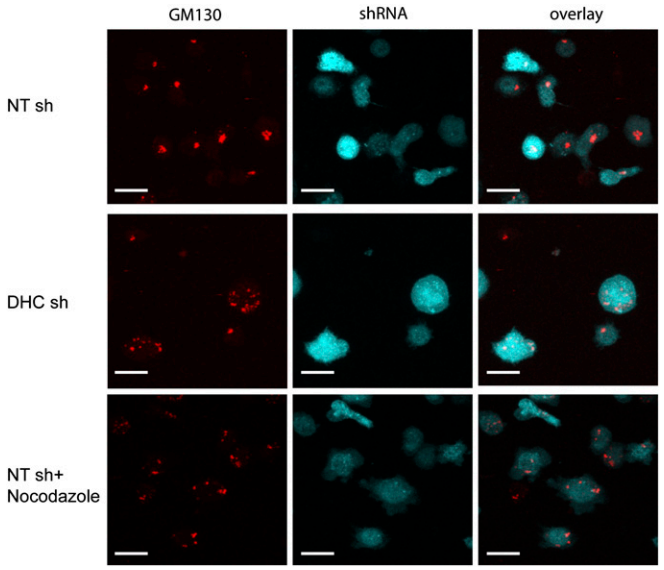


**Fig. S1.** DynHC shRNA induces Golgi dispersion in T cells. T cells (5C.C7) were transduced with either nontargeting (NT) shRNA or DynHC (DHC) shRNA and then fixed and stained for the Golgi marker GM130. Representative confocal images of the Golgi are shown, along with GFP fluorescence (marking shRNA expressing cells). In the lower images, NT shRNA-expressing cells were treated with 33 μM nocodazole to depolymerize microtubules, which also induces Golgi dispersion. (Scale bars: 10 μm.)

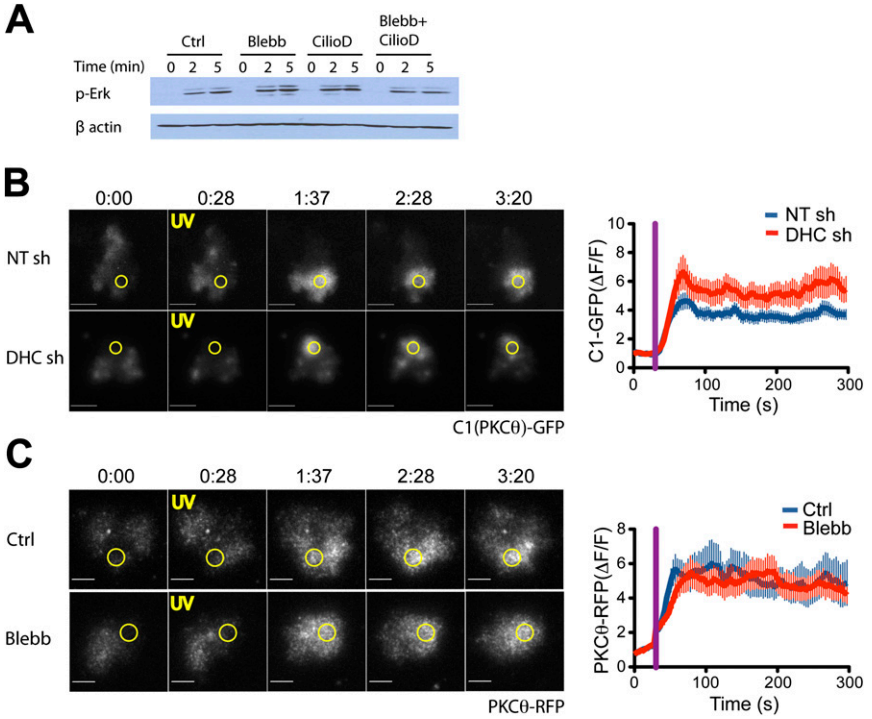


**Fig. S2.** Early T-cell activation is unaffected by inhibition of dynein and NMII. (*A*) T cells were mixed with antigen-loaded APCs in the presence of 50 μM blebbistatin, 50 μM ciliobrevin D, or vehicle control. At the indicated times, cell lysates were analyzed for Erk phosphorylation. β-Actin served as a loading control. (*B*) TCR-photoactivation experiments were performed using 5C.C7 T cells expressing a diacylglycerol (DAG) biosensor (the C1 domains of PKCθ fused to GFP) together with the indicated shRNAs. (*C*) Photoactivation experiments were performed using 5C.C7 T cells expressing PKCθ-RFP in the presence or absence of 50 μM blebbistatin. In *B* and *C*, representative montages are shown on the left, with the time of UV irradiation indicated by yellow text. Yellow circles denote the irradiated region. Time is shown as minutes:seconds above the montages. Quantification of fluorescence within the irradiated region was performed as described in Fig. 3. Purple lines denote UV irradiation, and error bars indicate SEM. At least nine cells were analyzed for each sample. (Scale bars: 5 μm.)

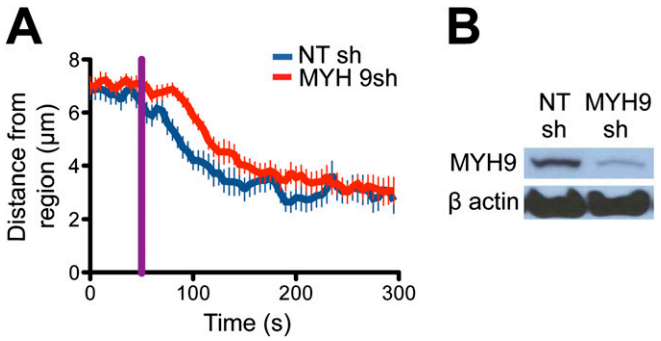


**Fig. S3.** NMII is required for optimal centrosome polarization. (*A*) Centrosome polarization in T cells expressing centrin-RFP and GFP-marked shRNA against MyH9 ($n \geq 15$ cells per sample). Results are presented as in Fig. 2. (*B*) Validation of MyH9 shRNA knockdown by immunoblot, with β-actin serving as a loading control. NT, nontargeting shRNA.

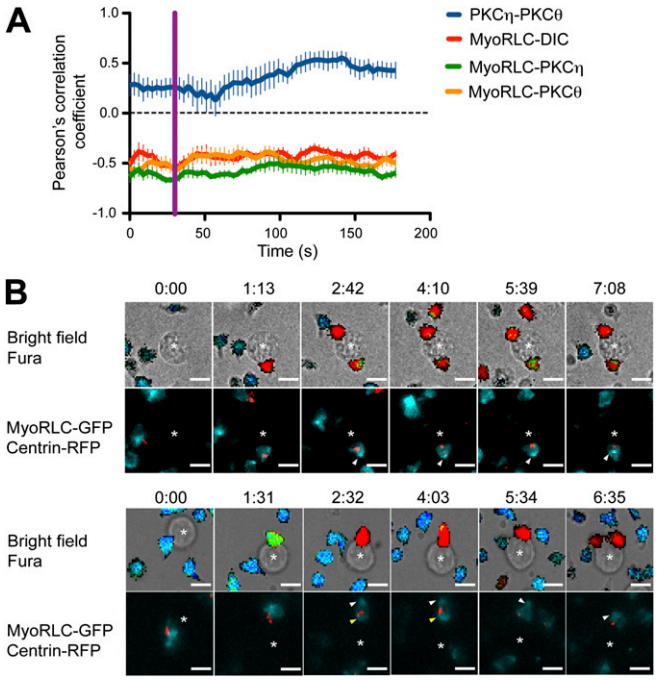


**Fig. S4.** NMII localization in photoactivation experiments and T cell–APC conjugates. (*A*) TCR-photoactivation experiments were performed using 5C.C7 T cells doubly transduced with MyoRLC-GFP and either DynIC-RFP (DIC), PKCθ-RFP, or PKCη-RFP. Overlap between the GFP and RFP probes in each experiment was quantified by PCC both before and after UV irradiation (indicated by the purple line). PCC > 0 indicates a positive correlation, and PCC < 0 indicates anti-correlation. For comparison, data collected from cells expressing PKCη-GFP and PKCθ-RFP (which are known to colocalize) are also included (blue line). At least 10 cells were analyzed for each curve. Error bars denote SEM. (*B*) T-cell blasts (5C.C7) expressing MyoRLC-GFP and centrin-RFP were loaded with the calcium indicator Fura-2 AM and mixed with antigen-loaded CH12 cells. Two representative time-lapse montages of conjugates are shown, with Brightfield Fura-2 images above (Brightfield-Fura) and GFP/RFP images below. Fura-2 images are pseudocolored, with warmer colors indicating higher intracellular $Ca^{2+}$ concentration. White asterisks denote the position of the APCs. White arrowheads indicate MyoRLC-GFP puncta at the sides and rear of the T cell. Yellow arrowheads indicate accumulation of MyoRLC-GFP at the IS, which we observed in a minority of conjugates. (Scale bars: 10 μm.)

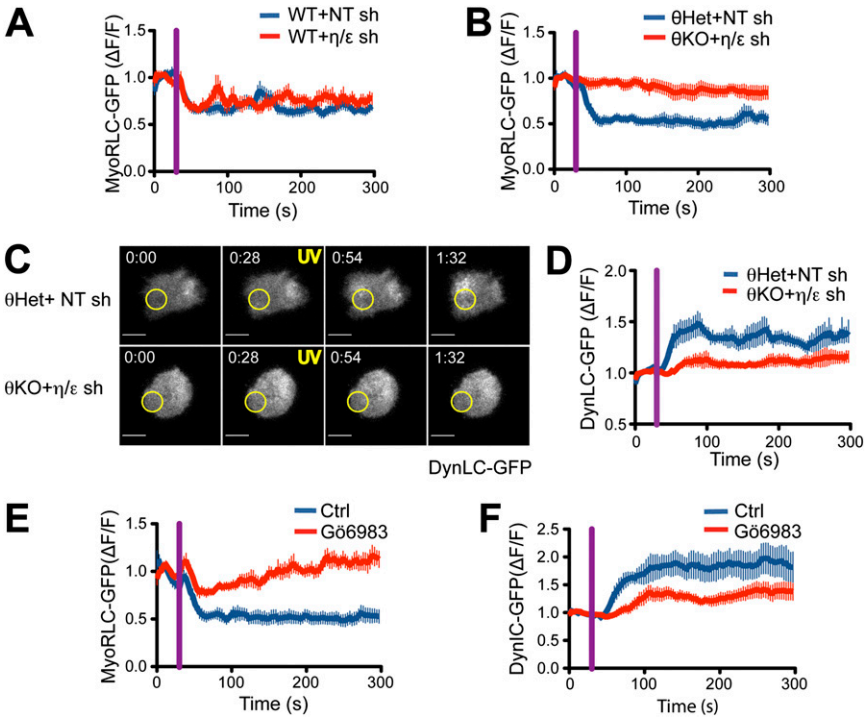


**Fig. S5.** NMII and dynein asymmetry is regulated by novel (n) PKCs. T cells (5C.C7) derived from PKCθ$^{+/+}$ (WT), PKCθ$^{+/-}$ (θHet), or PKCθ$^{-/-}$ (θKO) mice were transduced with either MyoRLC-GFP (*A* and *B*) or DynLC-GFP (*C* and *D*) together with the indicated shRNAs and used for photoactivation experiments. (*A*, *B*, and *D*) Quantification of NMII clearance and dynein recruitment ($n \geq 10$ cells for each sample). (*C*) Representative time-lapse montages comparing dynein recruitment in nPKC-sufficient and nPKC-deficient cells. The time of UV irradiation is indicated by yellow text, and the irradiated region is denoted by yellow circles. Time is shown on each image as minutes:seconds. (Scale bars: 5 μm.) (*E* and *F*) T cells (5C.C7) expressing either MyoRLC-GFP (*E*) or DynIC-GFP (*F*) were photoactivated and imaged in the presence or absence of 500 nM Gö6983. Graphs show NMII clearance and dynein recruitment ($n = 10$ cells for each sample). Quantification of NMII and dynein remodeling in *A*, *B*, and *D–F* was performed as in Fig. 3. Purples lines denote UV irradiation, and error bars indicate SEM.

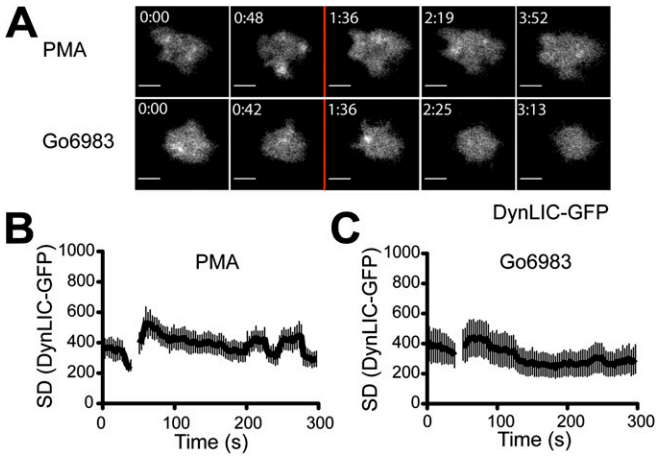


**Fig. S6.** Acute activation or inhibition of PKC activity has little effect on dynein distribution. T cells (5C.C7) expressing DynLIC-GFP were imaged in total internal reflection fluorescence (TIRF) and treated with 5 ng/mL PMA or 500 nM Gö6983 as indicated during time-lapse acquisition. (*A*) Representative time-lapse montages, with addition of reagents indicated by the red line. (Scale bars: 5 μm.) (*B* and *C*) Clustering of DynLIC at the membrane was quantified by calculation of the SD of the fluorescence signals for each cell ($n = 5$ cells per curve; see also *Materials and Methods*). The time of reagent addition is indicated by the gap in each curve. Error bars denote SEM.

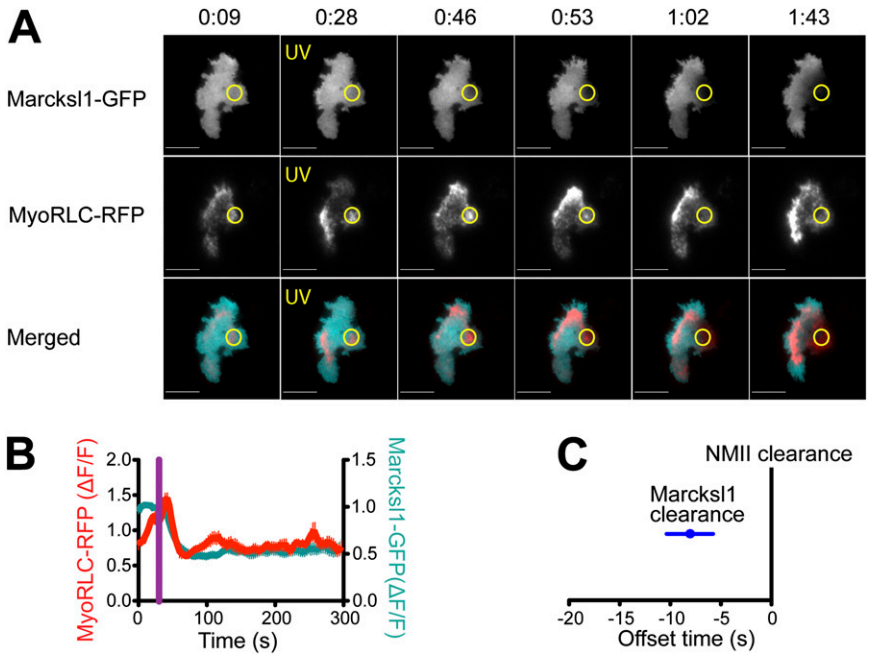


**Fig. S7.** NMII depletion correlates with PKC activity in single cells. TCR-photoactivation and TIRF-imaging experiments were performed using 5C.C7 T cells expressing Marcksl1-GFP together with MyoRLC-RFP. (*A*) Representative time-lapse montage, with the time of UV irradiation indicated by yellow text. Yellow circles denote the irradiated region. (Scale bars: 5 μm.) (*B*) Quantification of Marcksl1 and MyoRLC depletion from the irradiated region, performed as in Fig. 3. The purple line denotes UV irradiation. (*C*) Temporal offset between MyoRLC clearance and Marcksl1 clearance, calculated by cross-correlation analysis ($n = 8$ cells). Error bars indicate SEM.

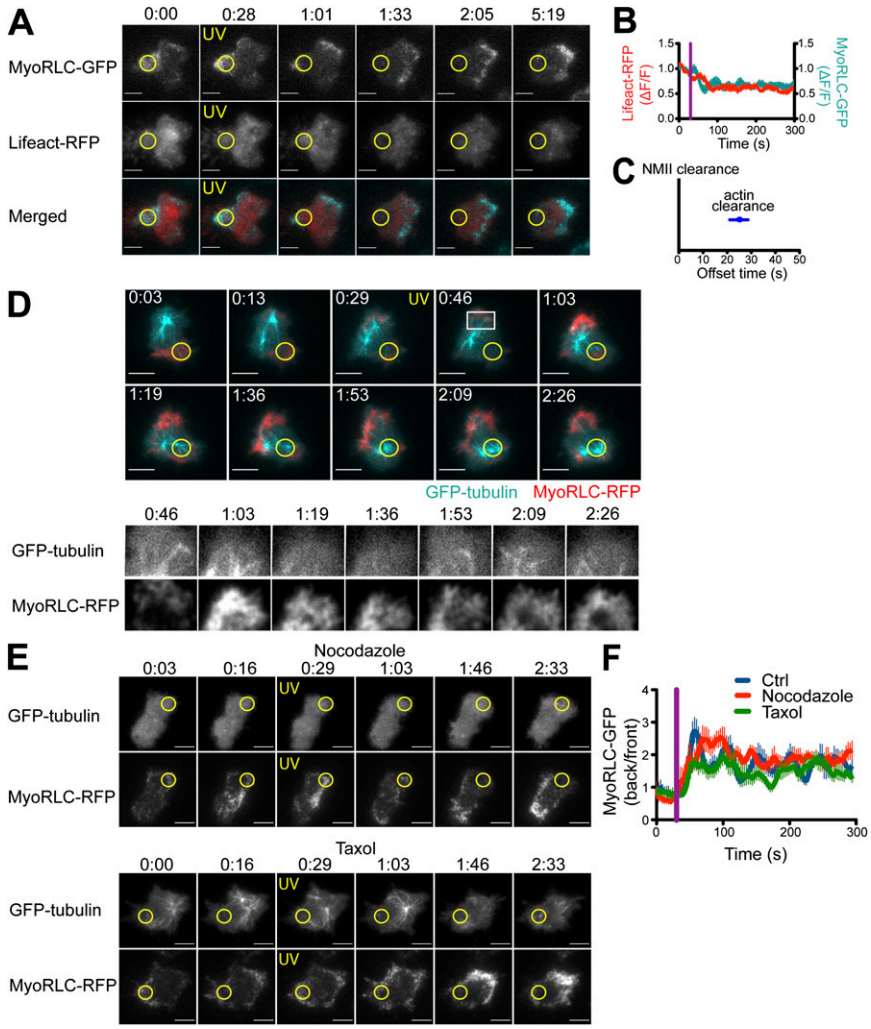


**Fig. S8.** NMII reorganization is independent of cortical actin remodeling and microtubule dynamics. (*A*–*C*) TCR-photoactivation and TIRF-imaging experiments were performed using 5C.C7 T cells expressing MyoRLC-GFP together with Lifeact-RFP. (*A*) Representative time-lapse montage, with the time of UV irradiation indicated by yellow text. Yellow circles denote the irradiated region. (Scale bars: 5 μm.) (*B*) Quantification of MyoRLC and Lifeact depletion from the irradiated region, performed as in Fig. 3. (*C*) Temporal offsets between MyoRLC clearance and Lifeact clearance, calculated by cross-correlation analysis ($n = 8$ cells). Error bars denote SEM. (*D*–*F*) TCR-photoactivation and TIRF-imaging experiments were performed using 5C.C7 T cells expressing MyoRLC-RFP together with GFP-tubulin. Cells were treated with 1 μM nocodazole or 100 nM taxol as indicated. (*D* and *E*) Representative time-lapse montages, with the time of UV irradiation indicated by yellow text. Yellow circles denote the irradiated region. (Scale bars: 5 μm.) The white square shown in the upper montage in *D* indicates the region enlarged in the lower montage. (*F*) MyoRLC asymmetry expressed as the MyoRLC-RFP MFI ratio between the back and the front of the T cell. Ten cells were analyzed for each condition. Error bars denote SEM.

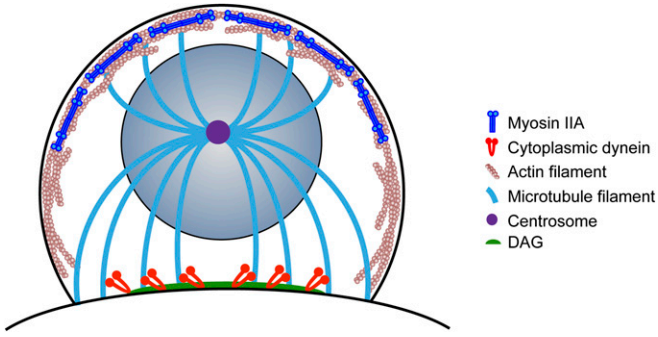


**Fig. S9.** Model for collaborative reorientation of the centrosome by dynein and NMII. Dynein molecules recruited by synaptic DAG accumulation are anchored at the IS and "pull" on the microtubule network. Meanwhile, NMII clusters at the distal end of the T-cell contract, generating forces that "push" the microtubule network toward the IS.

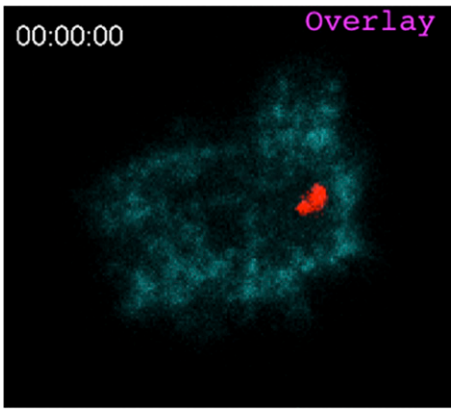


**Movie S1.** NMII clusters behind the centrosome as it reorients. T cells (5C.C7) expressing MyoRLC-GFP together with centrin-RFP were imaged (150× magnification) and UV-irradiated on glass surfaces coated with photoactivatable pMHC. A 15× time lapse of a representative experiment is shown, with MyoRLC TIRF signal on the left, centrin epifluorescence in the center, and the overlay on the right. Time is displayed (HH:MM:SS) in the upper left corner of each image. The region of UV irradiation is indicated by the green oval, and the time of irradiation is indicated by the appearance of yellow text.

Movie S1

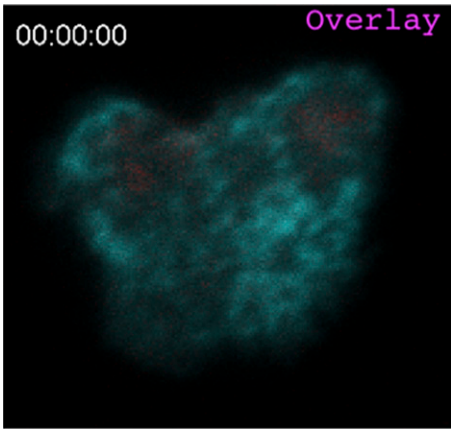


**Movie S2.** Dynein and NMII adopt reciprocal localization patterns. T cells (5C.C7) expressing MyoRLC-GFP together with DynIC-RFP were imaged (150× magnification) and UV-irradiated on glass surfaces coated with photoactivatable pMHC. A 15× time lapse of a representative experiment is shown, with MyoRLC TIRF signal on the left, DynIC TIRF signal in the center, and the overlay on the right. Time is displayed (HH:MM:SS) in the upper left corner of each image. The region of UV irradiation is indicated by the green oval, and the time of irradiation by the appearance of yellow text.

Movie S2

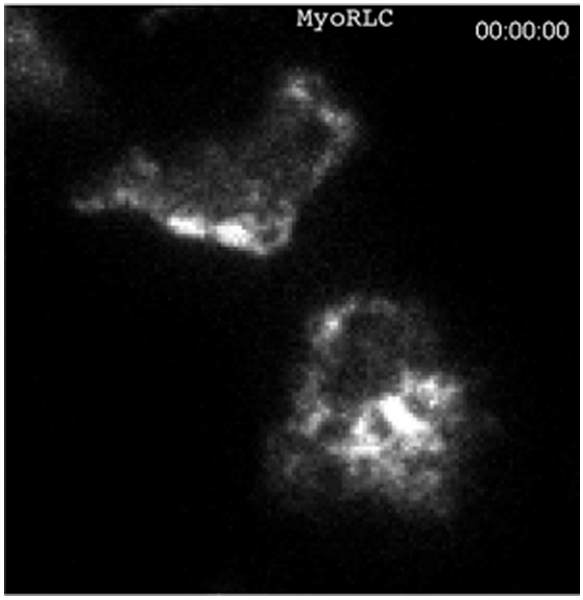


**Movie S3.** Acute PKC activation disrupts NMII clustering. T cells (5C.C7) expressing MyoRLC-RFP were imaged by TIRF microscopy (60× magnification) and treated with 5 ng/mL PMA to induce generalized PKC activation. A 15× time lapse of a representative experiment is shown, with the addition of PMA indicated by the appearance of yellow text. Time is displayed (HH:MM:SS) in the upper right corner of the image.

Movie S3

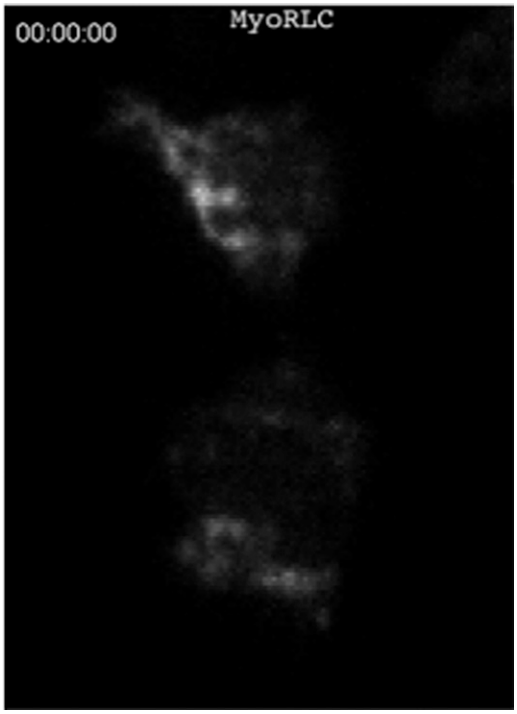


**Movie S4.** Acute PKC inhibition induces cortical NMII clustering. T cells (5C.C7) expressing MyoRLC-RFP were imaged by TIRF microscopy (60× magnification) and treated with 500 nM Gö6983 to inhibit PKC activity globally. A 15× time lapse of a representative experiment is shown, with the addition of Gö6983 indicated by the appearance of yellow text. Time is displayed (HH:MM:SS) in the upper left corner of the image.

Movie S4

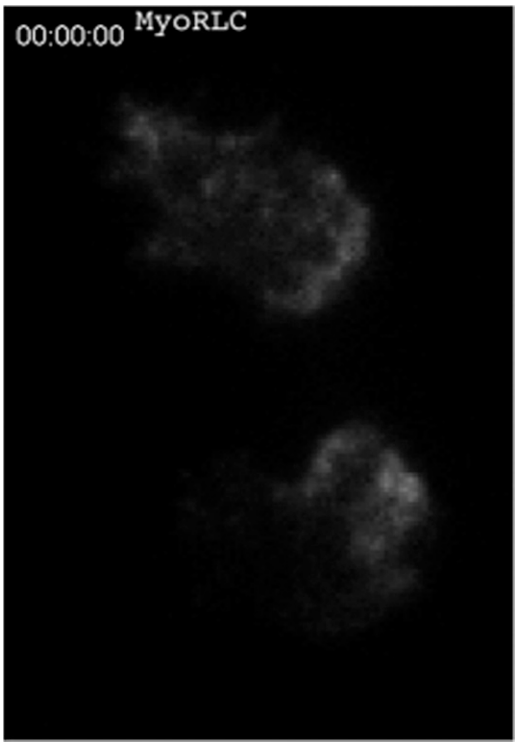


**Movie S5.** PKC inhibition blocks PMA-induced NMII dispersion. T cells (5C.C7) expressing MyoRLC-RFP were imaged by TIRF microscopy (60× magnification) and treated simultaneously with 5 ng/mL PMA and 500 nM Gö6983. A 15× time lapse of a representative experiment is shown, with the addition of PMA and Gö6983 indicated by the appearance of yellow text. Time is displayed (HH:MM:SS) in the upper left corner of the image.

Movie S5

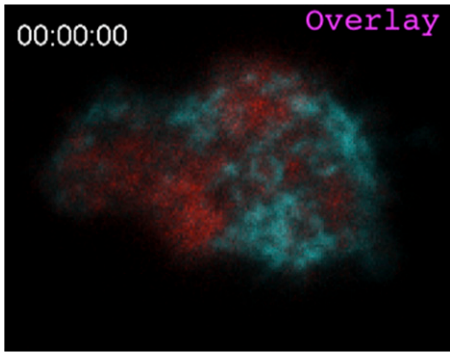


**Movie S6.** NMII and PKCη adopt reciprocal localization patterns. T cells (5C.C7) expressing MyoRLC-GFP together with PKCη-RFP were imaged (150× magnification) and UV-irradiated on glass surfaces coated with photoactivatable pMHC. A 15× time lapse of a representative experiment is shown, with MyoRLC TIRF signal on the left, PKCη TIRF signal in the center, and the overlay on the right. Time is displayed (HH:MM:SS) in the upper left corner of each image. The region of UV irradiation is indicated by the green oval, and the time of irradiation is indicated by the appearance of yellow text.

Movie S6

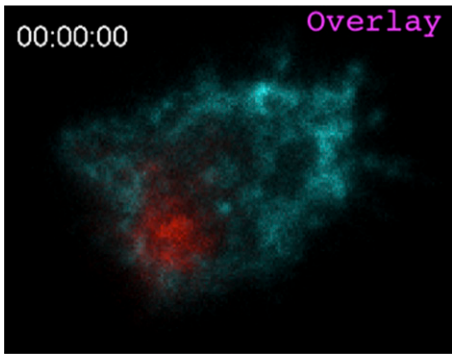


**Movie S7.** NMII and PKCθ adopt reciprocal localization patterns. T cells (5C.C7) expressing MyoRLC-GFP together with PKCθ-RFP were imaged (150× magnification) and UV-irradiated on glass surfaces coated with photoactivatable pMHC. A 15× time lapse of a representative experiment is shown, with MyoRLC TIRF signal on the left, PKCθ TIRF signal in the center, and the overlay on the right. Time is displayed (HH:MM:SS) in the upper left corner of each image. The region of UV irradiation is indicated by the green oval, and the time of irradiation is indicated by the appearance of yellow text.

Movie S7

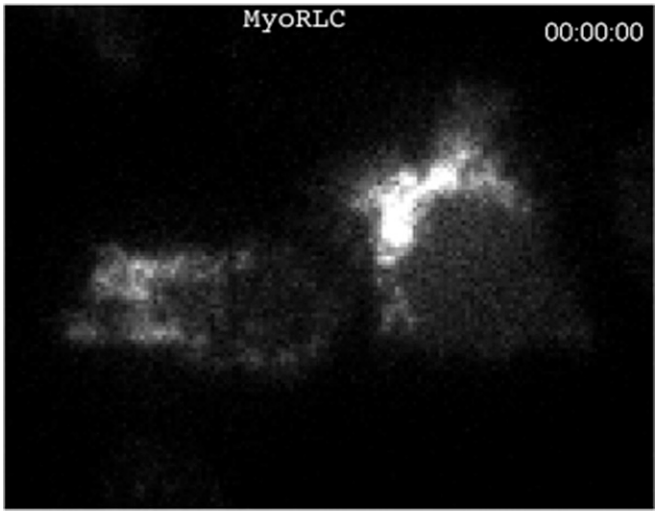


**Movie S8.** ROCK activity is required for cortical NMII clustering. T cells (5C.C7) expressing MyoRLC-RFP were imaged by TIRF microscopy (60× magnification) and treated with 50 μM Y27632 to inhibit ROCK. A 15× time lapse of a representative experiment is shown, with the addition of Y27632 indicated by the appearance of yellow text. Time is displayed (HH:MM:SS) in the upper left corner of the image.

Movie S8